Ionic arrest of segmental motion and emergence of spatio-temporal heterogeneity: A fluorescence investigation of (polyethylene glycol + electrolyte) composites

Biswajit Guchhait and Ranjit Biswas[a)]
Department of Chemical, Biological and Macromolecular Sciences, S. N. Bose National Centre for Basic Sciences, Block-JD, Sector-III, Salt Lake, Kolkata-700098, India

(Received 11 January 2013; accepted 5 March 2013; published online 21 March 2013)

Temperature dependent steady state and time resolved fluorescence measurements have been performed to explore the interaction and dynamics in polymer-electrolyte composite of the following general formula: [0.85 PEG + 0.15{f KNO_3+ (1−f) $LiNO_3$}], with f denoting fraction of potassium ion in the 0.15 mol electrolyte present in the medium. Poly(ethylene glycol) with number-averaged molecular weight of 300 (PEG300) has been employed as polymer and C153 as the fluorescent probe. Substantial excitation wavelength dependence of probe fluorescence emission in presence of electrolyte suggests presence of spatial heterogeneity which vanishes either upon raising temperature or removing the electrolyte. This has been interpreted as arising from the cation-induced arrest of polymer segmental motion. Temporal heterogeneity in these composites is manifested via fractional viscosity dependence of average solvation and rotation rates of the dissolved probe. Viscosity decoupling of these rates in composites is found to depend on cation identity and is also reflected via the corresponding activation energies. The degree of decoupling differs between solvation and rotation, inducing an analogy to the observations made in deeply supercooled liquids. In addition, conformity to hydrodynamic predictions is recovered by measuring f dependent solute rotation at higher temperatures. Several complimentary but different experiments are suggested to re-examine the mechanism proposed here, based on the fluorescence results, for the emergence of spatio-temporal heterogeneity in these composites and its disappearance either in the absence of any electrolyte or at higher temperatures. © *2013 American Institute of Physics*. [http://dx.doi.org/10.1063/1.4795583]

I. INTRODUCTION

Polymer electrolyte composites, or simply, polymer electrolytes constitute a subject of intense research because of their application potential in battery technology, dye sensitized solar cells, and chemical sensors.[1–4] These materials have drawn special attention because of their moderately large temperature stability (∼220–470 K)[1] and subsequent applicability in energy generation and storage devices. Ion transport is the key mechanism in battery technology and, as a result, nature of an added electrolyte crucially determines the efficiency of such power storage devices.[5,6] Previously, ionic conductivity aspects of polymer electrolytes have been explored for amorphous and crystalline states. Cation shows greater transference in crystalline form, whereas in amorphous form both ions show significant transference capability.[6,7] In these materials the ion transport is induced by local motion of polymer chain segment repeatedly creating new co-ordination sites into which the ion may then migrate.[6] These composites are low conducting materials and therefore attempts have been made to improve conductivity by changing the electrolyte.[8–10] Various new types of polymers and catalysts have also been synthesized for improving conductivity, chemical, mechanical, and dimensional stabilities.[11,12] Designing of flexible polymers with an aim to augment ion transport via segmental motion of the host polymer and subsequent experimental investigation have been the focus of several experimental studies performed earlier.[6,7,13,14]

Among various choices of polymers for preparing polymer-electrolyte composites, the ones based on polyethylene oxide (PEO) are the best and mostly studied[6–9,13–21] because PEO possessess large solubilising power for a wide variety of salts. It is now accepted that the cation (usually Li^+) of the added electrolyte coordinates with the host polymer molecules in both inter- and intra-molecular fashion.[1,6,13] Quasi-elastic neutron scattering (QENS) studies have revealed two dynamic processes in polymer-electrolyte composites where the faster one has been attributed to pure polymer and the slower to the formation of polymer-Li^+ complex. These facts correlate well with molecular dynamics simulations of similar system and the slow process has been explained in terms of heterogeneous dynamics.[14] QENS study has also revealed that the cations are co-ordinated with several ether oxygens of the same polymer molecule (intramolecular) quenching severely the segmental dynamics of the host polymer. When the ratio between the numbers of ether oxygens of polymer and metal ion (O:M) is ∼10:1, the extent of segmental motion reaches a minimum due to the formation of percolating network via cationic crosslink.[22] ^{1}H, ^{7}Li, and ^{19}F NMR studies of PEO electrolyte systems have provided a picture of relaxation of ions and polymer segments.[23] These

a)Author to whom correspondence should be addressed. Electronic mail: ranjit@bose.res.in.

experiments have shown that the cation motion is coupled with polymer segmental motion but the anion moves rather freely.[23] Different local environments of lithium cations due to preferential coordination in polyether poly(urethane urea) based polymer electrolytes has also been investigated by ^{7}Li magic angle spinning (MAS) NMR with high-power proton decoupling technique.[24] Furthermore, dielectric relaxation studies of polymer-electrolyte composites have indicated that the relative dielectric constant varies with frequency due to coupling of ion and polymer segmental motions.[18] Theoretical studies[15–17,25,26] have suggested that polymer chain dynamics plays a significant role in ion conduction mechanism. A molecular dynamics[17] study of polymer-electrolyte considering low molecular weight polymer has suggested that complexation of the cation as a polydentate ligand (chelate effect) with polymer molecules leads to the dissolution of the electrolyte into the host polymer. This study has also suggested that among different cations, Li^+ possesses the strongest affinity to be coordinated with ethereal oxygen atoms of the host polymer. Interestingly, simulated solvation dynamics for Na^+ in polymer has been found to be bimodal and belongs to the nonlinear response regime.[27]

Even though several aspects of polymer-electrolyte composites have been explored by a number of previous studies,[14,18,22,23,28–30] the impact of ion complexation with host polymer on the solution structure and the subsequent effects on relaxation dynamics have not yet been investigated in detail. Micro-domains created by the chelate effects of the cation (Li^+ or Na^+) will give rise to microscopic heterogeneity which will subsequently be reflected in the relaxation dynamics occurring in these complex media. This micro-heterogeneity can indeed be detected via the excitation wavelength (λ_{exc}) dependence of the steady state fluorescence emission of a solute probe possessing shorter excited state lifetime than the stability time of the fluctuating micro-domains. In addition, the proposed quenching (partial or full) of the segmental motion through ion complexation will be reflected via slower average rate of solute solvation or rotation polymer-electrolyte composites compared to those in the host polymer in the absence of any electrolyte. A temperature dependent study then should be able to reveal in greater detail the heterogeneity aspects and the nature of solute-solvent interaction in these composite materials. In fact, this is the theme of the present study. We would like to mention here no fluorescence investigation as discussed above exists except some reports on pure short chain polymers.[31,32] Thus, our proposed study is an attempt to better understand the solution structure and dynamics in low molecular weight based polymer-electrolyte systems in liquid state. Note the relaxation dynamics of aqueous solution of polymer solution using a fluorescence solute[33,34] have revealed biphasic solvation dynamics with widely separated timescales. Aqueous solution of triblock copolymer, P123 gel, has also been studied via fluorescence method and a marked red edge excitation shift (REES) has been revealed.[35] However, none of the studies investigate the ion effects and impact of segmental motion on relaxation dynamics in polymer matrix systems.

In this paper, we have studied the fluorescence Stokes shift dynamics and rotational relaxation of a dipolar solute

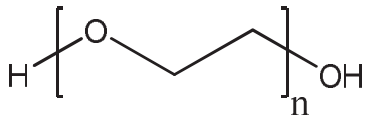

Polyethylene Glycol (PEG)

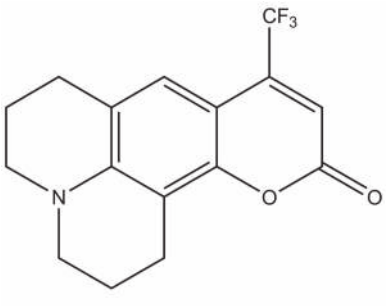

Coumarin 153 (C153)

FIG. 1. Chemical structures of polyethylene glycol (PEG) and Coumarin 153 (C153).

(C153) in polymer-electrolyte composites based on polyethylene glycol (PEG) and lithium/potassium nitrate (Li/KNO_3), and compared with the results obtained for pure PEG. Chemical structures of PEG and C153 are shown in Fig. 1. Note PEG is an example of hydrophilic block copolymer (lower homolog of PEO) which has many technological and biochemical applications.[36] We have considered the following polymer-electrolyte composite: $[0.85\text{PEG} + 0.15\{f\text{LiNO}_3 + (1-f)\text{KNO}_3\}]$. The choice of this composition is motivated by the following reasons. First, PEG-electrolyte composite with the above general formula has already been characterized via measurements of various physico-chemical parameters.[37] Second, the effects of cation identity on solution dynamics at a fixed concentration can be studied. This is important because solute-medium dynamical coupling might be different even at a fixed electrolyte concentration due to disparate mobilities of Li^+ and K^+. The scenario becomes even more interesting because presence of more than one alkali metal cations in a mixture is known to produce large length-scale jump motions and cooperative blockage in silicate glasses[38(a)] and (amide + electrolyte) deep eutectics.[38(b)] These non-Gaussian characteristics are expected to substantially modify solute-medium coupling. Third, spatial heterogeneity is expected to be different for these two cations as their complexation abilities are different.[17] The present study can re-examine this proposition by carrying out both steady state and time-resolved fluorescence measurements.

II. EXPERIMENTAL DETAILS

Laser grade C153 (Exciton) was used as received. Polyethylene glycol of number-averaged molecular weight 300 (PEG300), and AR grade $LiNO_3$ and KNO_3 (Sigma-Aldrich) were also used as received. The experimental solutions were prepared by mixing of required amount of

electrolyte/s with PEG at around 298 K. Proper care was taken to ensure complete dissolution of the added electrolyte and to avoid moisture absorption. Temperature of the sample chamber was maintained by circulating pre-heated water (Julabo, Model F32). Temperature dependent viscosities of PEG were measured by using an AMVn automated micro-viscometer from Anton Paar (falling ball method).

Steady-state absorption and emission spectra were collected using a UV-visible spectrophotometer (UV-2450, Shimadzu) and a fluorimeter (Fluoromax-3, Jobin-Yvon, Horiba), respectively. Solvent blank spectra were subtracted prior to analysis. All samples were excited at their respective absorption maxima for steady state fluorescence measurements. The time-resolved measurements were performed using a time correlated single photon counting (LifeSpec-ps, Edinburgh Instruments, U. K.) setup fitted with a diode laser producing 409 nm excitation light. The instrument response function (IRF) measured using water was found to be $\leq$70 ps. Time-resolved emission spectra (TRES) were synthesized from the intensity decays at ~18–20 equally spaced wavelengths across the steady state emission spectrum (of dissolved C153) for each of the samples by following the method discussed in detail in Refs. 39–41. Solvation response function was then constructed as follows:[42] $S(t) = \{\nu(t) - \nu(\infty)\}/\{\nu(0) - \nu(\infty)\}$, where $\nu(x)$ represents the fluorescence frequency at time t, 0, and ∞, respectively. We used peak frequency values of the TRES to determine $S(t)$. Average solvation times were then obtained via time-integrating the measured $S(t)$ which were found to be bi-exponential functions of time:

$$\langle \tau_s \rangle = \int_0^\infty dt S(t) = \int_0^\infty dt \sum_{i=1}^{2} a_i \exp(-t/\tau_i)$$
$$= (a_1\tau_1 + a_2\tau_2) \text{ with } (a_1 + a_2) = 1.$$

Time-resolved fluorescence anisotropy ($r(t)$) measurements were carried out following the protocol discussed in Refs. 39–41 and using the iterative reconvolution for simultaneous fitting of the parallel $\{I_{para}(t)\}$ and the perpendicular $\{I_{perp}(t)\}$ decays.[43–45] The geometric factor (G) was obtained by tail matching and found to be 1.15 $\pm$ 0.10. Normalized $r(t)$ decays were also found to fit bi-exponential functions of time and average rotation times were obtained as follows: $\langle \tau_r \rangle = \int_0^\infty dt[r(t)/r(0)] = \int_0^\infty dt \sum_{i=1}^{2} a_i \exp(-t/\tau_i) = (a_1\tau_1 + a_2\tau_2)$, where $r(0)$, denoting the initial anisotropy, was fixed at 0.376[43] (for all the samples studied here), and $(a_1 + a_2) = 1$.

III. RESULTS AND DISCUSSION

A. Ion-induced heterogeneity: Signature from steady state spectral measurements

Steady state absorption and emission spectra of C153 in [0.85 PEG + 0.15 $\{f KNO_3 + (1-f)\ LiNO_3\}$] mixtures were collected at various fractions (f) of KNO_3. As a representative example, absorption and emission spectra of C153 at $f = 0.2$ are shown in the upper panel of Fig. 2 and compared with those in pure PEG. Note the electrolyte-induced redshift

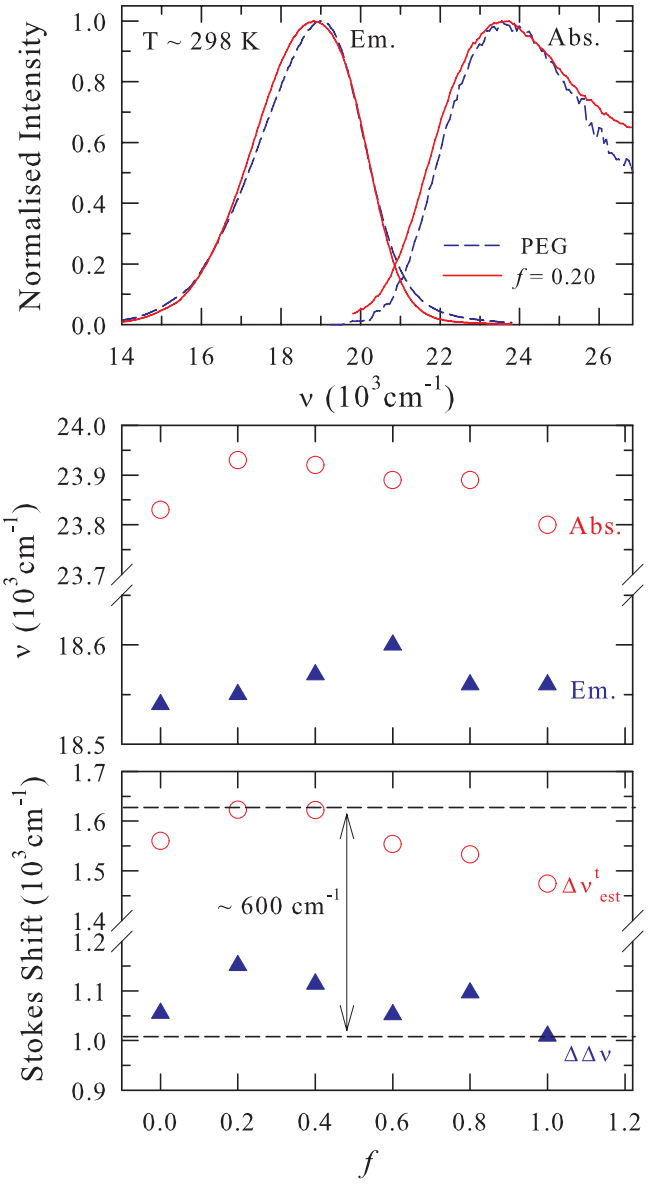

FIG. 2. Representative steady state absorption and emission spectra of the dissolved solute, C153, in [0.85PEG + 0.15$\{f KNO_3 + (1-f)\ LiNO_3\}$] mixture at $f = 0.20$ and in PEG are shown in the upper panel. Fraction of K^+ ion concentration (f) dependent frequencies (absorption and emission) and steady state relative ($\Delta\Delta\nu$) and estimated dynamic ($\Delta\nu^t_{est}$) Stokes shifts at 298 K are presented in the middle and lower panels, respectively. Measured frequencies are better than $\pm$150 cm^{-1}.

of the spectral position (in energy) at this electrolyte concentration is small (~300 cm^{-1}), indicating a minimal change in local polarity (around the probe molecule) upon addition of electrolyte at this concentration over that in pure PEG. Note this amount of electrolyte-induced emission shift is comparable to that observed for uni-univalent electrolyte solutions in solvents of much higher static dielectric constant (ε_0)[46,47] and much less than expected (based on electrolyte-induced shift in solutions of low polarity solvents)[46–50] given that $\varepsilon_0 \approx 15$ for the PEG300[51] used in this work. The observed less-than-expected shift in this polymer-electrolyte composite is therefore suggestive of complexation of ion (here K^+) with the PEG molecules which prevents the ions to interact directly with the dissolved dipolar solute, C153.

Absorption and emission frequencies, presented in the middle panel as a function of KNO_3 fraction, exhibit non-monotonic K^+ ion concentration dependencies. Even though the extent of non-monotonicity is very weak and within our instrumental resolution (~150 cm^{-1}), the dependence is systematic and reproducible. In addition, this non-monotonic dependence is qualitatively similar to our earlier observations for (acetamide + K/NaSCN) deep eutectics which was explained in terms of packing and medium heterogeneity.[39] The non-monotonicity is further extended into the K^+ ion concentration dependence of the estimated dynamic ($\Delta\nu^t_{est}$)[52] and relative steady state ($\Delta\Delta\nu$) Stokes shifts. An important point here is that $\Delta\nu^t_{est}$ in these composites is larger by ~600 cm^{-1} than $\Delta\Delta\nu$, suggesting environmental relaxation much slower than the excited state population relaxation. In fact, $\Delta\nu^t_{est}$ being larger than $\Delta\Delta\nu$ is rather a general observation in media where ion-solvent complexation occurs and the resultant ion-solvent composite body moves at a rate slower than depopulation of the solute from its excited state.[39,41,47] Interestingly, presence of such "longer-lived" environment renders spatial heterogeneity in solution structure that may be probed by the excitation wavelength (λ_{exc}) dependence of fluorescence emission of a dissolved solute. This is what we describe next.

Figure 3 depicts the λ_{exc} dependence of the peak frequency (ν_{em}) of fluorescence emission of C153 dissolved in PEG-electrolyte composite at two different K^+ ion concentrations, $f = 0.2$ and 0.8. λ_{exc} dependent ν_{em} obtained for pure PEG (that is, in the absence of any added electrolyte) is also shown for comparison. Note that ν_{em}, presented in the upper panel, shows slightly larger (~600 cm^{-1}) redshift at $f = 0.2$ than that (~500 cm^{-1}) at $f = 0.8$ upon changing λ_{exc} from the highest (370 nm) to the lowest (480 nm) energies. The observed similar magnitude of emission shift at these two different K^+ ion concentrations suggests near-equivalence in the extent of spatial heterogeneity caused via complexation of K^+ and Li^+ with the polymer (PEG) molecules. This amount of spectral shift is, however, accompanied by spectral narrowing by ~1000–1400 cm^{-1}, indicating a fairly inhomogeneous distribution of relatively "longer-lived" solvation environments around the excited C153 (excited state life-time, τ_{life} ~4–5 ns).[42] This is to be contrasted with the λ_{exc} dependence of pure PEG in the absence of any electrolyte where ν_{em} experiences a shift of only ~200 cm^{-1} for the same range of λ_{exc}. Excitation wavelength dependence of solute emission has also been encountered, with a varying degree, in deep eutectics,[39,41] ionic liquids,[53–55] and reverse micelles.[44] The observed stronger λ_{exc} dependence of ν_{em} in polymer-electrolyte composite than in PEG can therefore be regarded as an evidence in favour of ion-induced spatial heterogeneity in these complex systems where the cation complexes with the host polymer. Experimentally measured very low transference number for singly charged cation in polymer electrolyte[56] also provides further support to such ion-polymer complexation.

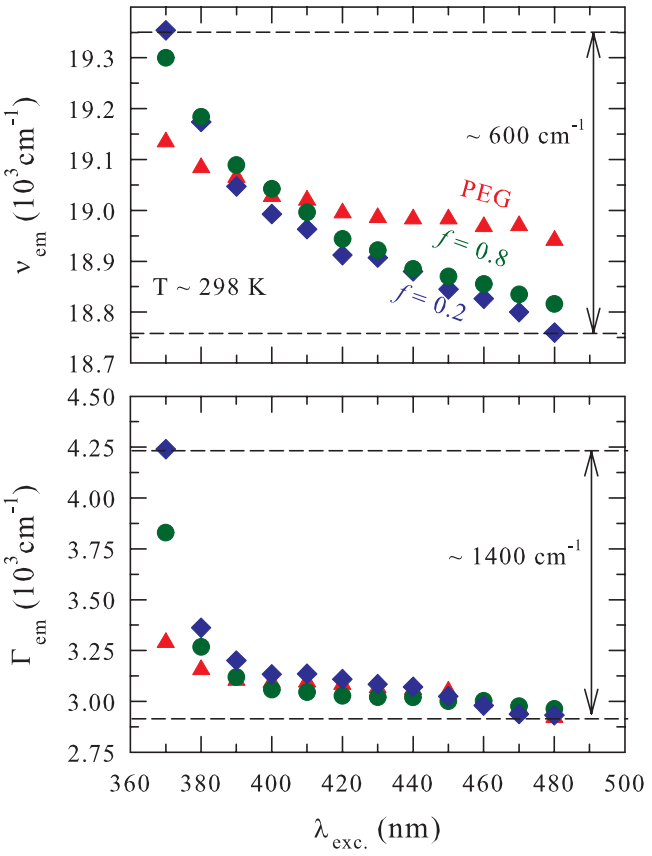

FIG. 3. Excitation wavelength dependence (λ_{exc}) of emission peak frequencies (ν_{em}, upper panel) and spectral widths (Γ_{em}, lower panel). Spectral width means full-width-at-half-maximum (FWHM). The uncertainty in frequencies is better than ±150 cm^{-1}.

B. Ion-induced heterogeneity: Footprints in time-resolved measurements

1. Dynamic Stokes shift measurements

For all the compositions of PEG-electrolyte composites considered here and the PEG (that is, in the absence of electrolyte), time-resolved fluorescence intensity decays collected at magic angles are characterized by what is commonly regarded as the signature of Stokes shift dynamics; only decay at blue (higher energy, relative to the peak of the steady state emission spectrum) wavelengths and rise followed by decay at the red (lower energy) wavelengths. A representative example is provided in Fig. 4 where decays at blue and red wavelengths for C153 in PEG and in polymer-electrolyte composites at $f = 0$ and $f = 1$ are shown along with tri-exponential fit parameters. Note the intensity decays at or around the peak wavelengths fit to bi-exponential functions. As evident, the presence of electrolyte is manifested via the lengthening of the time constants tabulated as insets inside these panels. These unconstrained fits also reflect near-constancy of the excited state lifetime of C153 (~4–5 ns)[42] with f. In addition, solvent relaxation timescales are the slowest at $f = 0$ where only Li^+ is present. This is probably due to stronger complexation ability of Li^+ with polymer molecules. This aspect has also been reflected in the slightly larger λ_{exc} dependent shift of ν_{em} in the Li^+ enriched polymer-electrolyte composite than in the composition with larger K^+ concentration (see Fig. 3).

Subsequently, the dynamic Stokes shift, $\Delta\nu^t_{obs}$, has been obtained after constructing the TRES from these intensity decays.[57] The representative time resolved emission spectra,

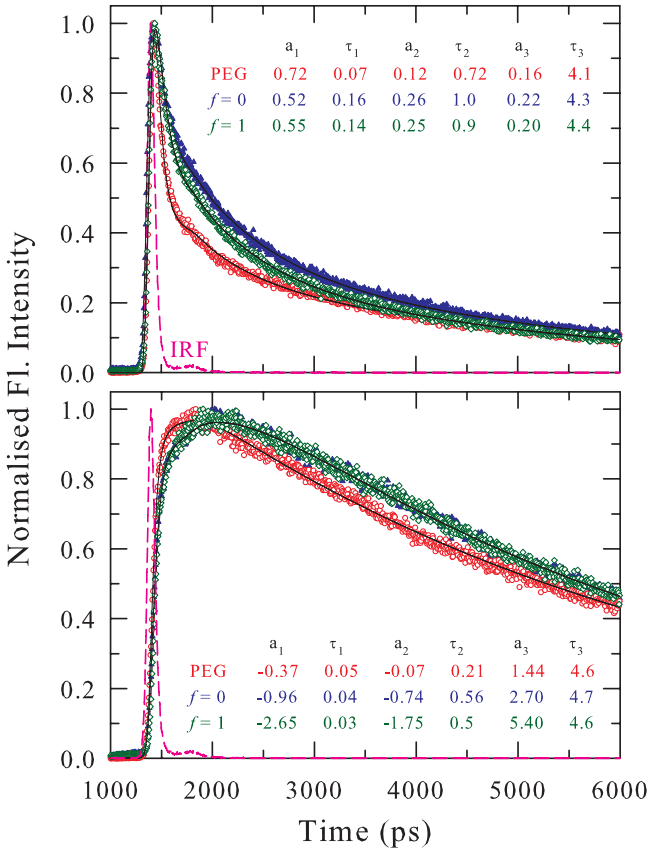

FIG. 4. Wavelength dependent emission intensity decays of C153 at ~298 K in PEG and in [0.85PEG + 0.15{f KNO$_3$ + (1 − f)LiNO$_3$}] composite with f = 0.0 and 1.0 at blue and red wavelengths, respectively. Symbols denote the experimental data and solid lines represent fits through them. Instrument response function (IRF) is also shown in both of the panels. Insets provide the amplitudes (a_is) and time constants (τ_is) required to fit these decays. Note the time constants are in the unit of nanosecond.

so constructed for C153 in polymer-electrolyte composite at f = 0.4 are shown in Fig. S1 of the supplementary material.[58] The measured dynamic shift values are then determined as $\Delta\nu^t_{obs} = \nu(t=0) - \nu(t=\infty)$, using the peak frequency of the TRES at these two points of time. The broad time resolution (~70 ps) employed in the present experiments does not allow detection of the "true" $\nu(t=0)$ and thus a portion of the total dynamic shift is missed. We have used a well-known approximate method[52] to estimate the total dynamic shift ($\Delta\nu^t_{est}$) for pure PEG and PEG-electrolyte composites, and summarized them in Table I along with $\Delta\nu^t_{obs}$ and the missing portions. Note the magnitude of $\Delta\nu^t_{est}$ for PEG in the absence of electrolyte is close to the shift detected for pentanol[42] (ε_0 = 13.9) and in good agreement with earlier results.[31] The observed shifts are, however, ~30% less than the estimated ones and in ~1000 cm^{-1} range. The fact that ~30% of the total shift in these systems has remained undetected also compares well with the observation that a significant portion (~35%) of the dynamics of pentanol can be characterized by a timescale of ~20 ps.[42] Interestingly, addition of electrolyte reduces $\Delta\nu^t_{est}$ values (obtained for pure PEG) by ~150–250 cm^{-1}, a trend opposite to what has been observed in electrolyte solutions of common polar solvents.[47] Even though such a small variation in $\Delta\nu^t_{est}$ may originate

TABLE I. Estimated ($\Delta\nu^t_{est}$) and observed ($\Delta\nu^t_{obs}$) dynamic Stokes shifts and percentage of missing portion of the total dynamics for C153 in PEG and in [0.85PEG + 0.15{fKNO$_3$ + (1−f)LiNO$_3$}] composites at 298 K.

System	$\Delta\nu^t_{est}$ (10^3 cm^{-1})	$\Delta\nu^t_{obs}$ (10^3 cm^{-1})	% missed
PEG	1.724	1.135	34
	0.85PEG + 0.15{fKNO$_3$ + (1−f)LiNO$_3$}		
f = 0.00	1.560	1.013	35
0.20	1.642	1.095	33
0.40	1.603	1.091	32
0.60	1.550	1.097	29
0.80	1.550	1.017	34
1.00	1.474	1.026	30

from mechanism other than medium reorganization, a role for the ion-polymer complexation and the subsequent inhibition of ion-solute interaction[59,60] cannot be ruled out. The temperature dependence of dynamic shift has also been investigated for pure PEG and in PEG-electrolyte composites at two representative K$^+$ ion concentrations (f = 0.2 and 0.8). The results, summarized in Table S2,[58] indicate decrease of shift with increase in temperature which may be attributed to the reduction of ε_0 with temperature for PEG.[61]

The effects of electrolyte and K$^+$ concentration on solvation response function are shown in the upper panel of Fig. 5 and the dependence on temperature at a fixed K$^+$ concentration (f = 0.8) is depicted in the lower panel of the same figure. These decays are biphasic and can be adequately described by a sum of two exponentials. Both addition of electrolyte to PEG and alteration of solution temperature are expected to affect the solvation rate as they introduce substantial changes in medium viscosity (see Table S3)[58] which regulates the solvation rate at long-time via diffusion.[62] However, isotopic substitution studies have suggested that diffusive modes involve only the polymer end-groups, not the entire body diffusion, which regulates the long-time solvation rate in PEG.[63] Dielectric relaxation (DR) measurements also support this view as the slowest DR time constant in PEG has been ascribed to the relaxation of the intermolecular hydrogen-bond (H-bond) network involving the polymer end-groups.[31] Parameters required to fit the measured f dependent $S(t)$ decays summarized in Table II reveal that the total solvation response in PEG and PEG-electrolytes is characterized by two components: a relatively faster component with time-constant in ~50–100 ps range, followed by a slower nanosecond (~800–1500 ps) component. The slow nano-second component in bulk electrolyte solutions of low polarity solvent has earlier been explained in terms of diffusive cation-solvent exchange in the first solvation shell of the excited solute.[46(c)] Such a mechanism here is unlikely as steady state spectral shifts measured here and simulations performed earlier[17] indicate severe restriction of cation movement via complexation. A comparative femtosecond Raman-induced Kerr effect spectroscopic (RIKES) study between ionic liquids and concentrated electrolyte solutions of PEG also indicates stronger PEG-Li$^+$ interaction.[64(a)] It is evident that the slower of the two time constants is further slowed down upon addition of electrolyte and exhibits a clear f dependence.

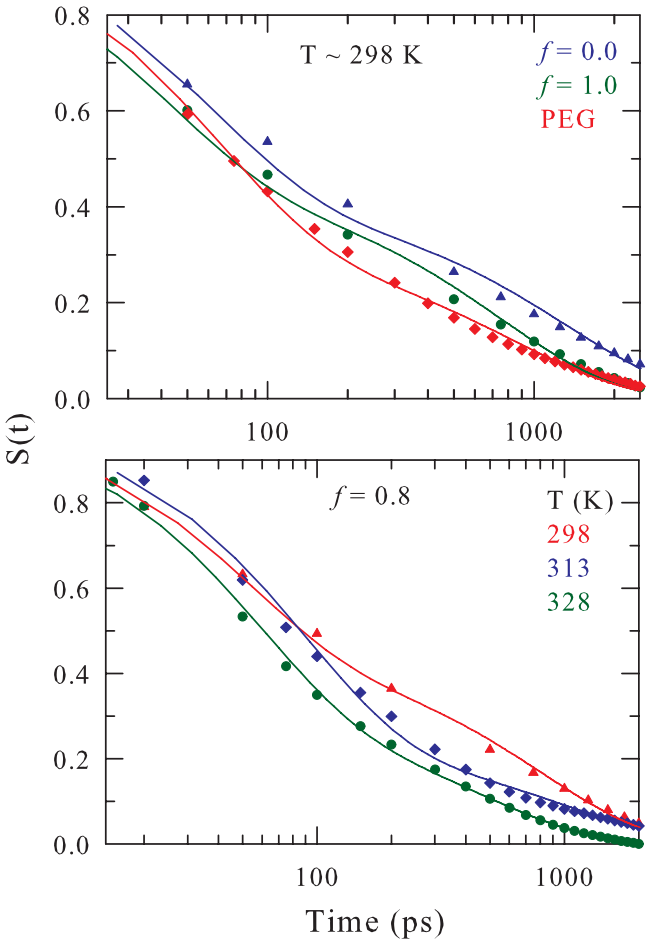

FIG. 5. Effects of electrolyte on solvation response function (upper panel) and temperature (lower panel). The polymer-electrolyte composite [0.85 PEG + 0.15{f KNO_3 + (1−f) $LiNO_3$)], with $f = 0.0$ and 1.0 has been considered to show the electrolyte and K^+ ion concentration effects using C153 as probe at 298 K. Solvation response at T(K) > 328 could not be measured because the dynamics became too fast to make any meaningful detection by the time resolution employed.

Interestingly, this time constant is the longest at $f = 0$ where both Li^+ concentration and solution viscosity are the maximum. We next ask: what gives rise to these two widely different timescales and how the above observation as a whole is related to the electrolyte-induced arrest of segmental motion?

TABLE II. Decay characteristics of solvation response function, $S(t)$, of C153 in PEG and in [0.85PEG + 0.15{$f$$KNO_3$ + (1−f)$LiNO_3$}] composites at 298 K.

System	η (cP)[a]	a_1	τ_1 (ps)	a_2	τ_2 (ps)[b]	$\langle\tau_s\rangle$ (ps)
PEG	70.44	0.67	62	0.33	845	320
	0.85PEG + 0.15{$f$$KNO_3$ + (1−f)$LiNO_3$}					
$f = 0.00$	144.4	0.63	100	0.37	1538	632
0.20	140.7	0.64	67	0.36	1430	558
0.40	130.6	0.63	50	0.37	1250	494
0.60	128.6	0.61	53	0.39	1111	465
0.80	125.6	0.64	73	0.36	1110	446
1.00	117.4	0.66	64	0.34	1052	400

[a]Viscosity values at various fractions (f) of K^+ ion concentration are from Ref. 37.
[b]Uncertainties associated with a_i and τ_i are, respectively, ±5% and ±10% of the reported numbers (estimated based upon limited datasets).

PEG systems possess low frequency (~100 cm^{-1}) intermolecular modes[64(b)] which may couple to dynamic solvation process and produce ultrafast polar solvation response.[62,65] Earlier simulations[27] and measurements[66] indeed confirm the presence of a sub-picosecond solvation component in polyether systems (related to PEG300 considered here) which is completely missed in the present experiments due to broad time-resolution employed. DR measurements also report a timescale of ~3 ps originating from the rotation of non-H-bonded hydroxyl (–OH) groups[51] in PEG300 which can produce ultrafast solvation response.[62,67] These DR measurements have also reported a time constant of ~100 ps and assigned to intramolecular segmental motion ("crankshaft" mode). This contribution of the segmental motion is reflected in the present experiments via the emergence of ~50–100 ps timescale. Earlier solvation measurements of C153 in polyether[32] and PEG300[31] also assign this timescale to the intramolecular segmental modes of the polymer. The present experiments further support this view as Li^+ slows down this component considerably via complexation with ether oxygens of surrounding polymer molecules. Computer simulations have indeed found evidences of such interaction while studying solvation response in flexible polyether by using Na^+ as probe.[27] Addition of water in polyether has been found to lengthen the overall relaxation time constant in DR measurements and this observation has been interpreted in terms of reduction (or partial arrest) of the crankshaft-like segmental mode.[68] Note Li^+ can also form complexes via interacting with the end –OH groups of the polymer molecules, effectively inhibiting the ability of the latter (–OH groups) to participate in the H-bond network fluctuation. This will further lengthen the slowest reorientation timescale of PEG (~300 ps)[51] which is the source for the nanosecond solvation response observed here in polymer-electrolyte composites and in the absence of electrolyte. Li^+ being smaller than K^+ should be able to form stronger complex and this is reflected in the longer time constant (Table II) becoming faster upon gradual replacement of the relatively smaller alkali metal cation by the larger one. Note the arrest of segmental motion by the alkali metal cation, as suggested earlier,[32] can also contribute to lengthening of the slowest reorientation timescale (and thus to solvation response) via affecting the flexibility of the polymer backbone.

The coupling of medium viscosity to solvation response in PEG requires a discussion as polymer fragment movements, not the whole body motion, are believed to carry out the solvation process of an excited probe. As viscosity of PEG has been shown to depend linearly on molecular weight,[31] the observed proportionality between viscosity and the slowest time constant may be construed as mass dependence of solvation rate. This is counter-intuitive as mass dependence is expected for the short time dynamics which is either inertia-driven or controlled by the collective intermolecular solvent modes such as libration and vibration.[62] Interestingly, deuterium substitution has produced only ~1% increase of viscosity resulting in ~20% slowing down of the long-time decay of the measured polar solvation response in PEG300.[63]

TABLE III. Activation energies (E_a) obtained from the Arrhenius plots for temperature dependent viscosity, and solvation and rotation times of C153 in PEG and in [0.85PEG + 0.15{fKNO$_3$ + (1−f)LiNO$_3$}] composites (with $f = 0.2$ and 0.8 only) at 298 K. Uncertainty associated with the E_a values is ±5% of the reported numbers.

System	E_a^{η} (KJmol^{-1})	$E_a^{\langle\tau_s\rangle}$ (KJmol^{-1})	$E_a^{\langle\tau_r\rangle}$ (KJmol^{-1})
PEG	31.66	42.04	42.17
	0.85PEG + 0.15{fKNO$_3$ + (1−f)LiNO$_3$}		
$f = 0.2$	36.82	24.89	30.30
0.8	36.14	18.19	28.73

Although similar slowing down is also found for solvation response in water upon deuteration,[69,70] the increase in viscosity has been ∼20% which proportionately lengthened the slowest dielectric relaxation time of water.[62] This contrast suggests that the frictional response of PEG300 derives a major contribution from sources other than macroscopic viscosity, and breaking and reformation of intermolecular H-bond (network fluctuation) by the end –OH groups is one such source. Alteration of the propensity of this local network fluctuation via complexation of hydroxyl groups with alkali metal ions will lead to enhanced resistance to medium rearrangement in response to solute excitation. Temperature dependence of solvation response will reflect this via less increase of solvation rate than that of viscosity. This has indeed been observed in our temperature dependent measurements and the results are summarized in Table S4.[58] Data tabulated here indicate that for changing temperature from 298 K to 318 K of PEG solution in the absence of electrolyte, the long-time constant becomes faster by a factor of ∼4 whereas the viscosity reduces by a factor of ∼2.5. Similar changes in viscosity are observed in the presence of electrolyte at $f = 0.2$ and 0.8 for the same temperature increase but the long-time constant becomes approximately twice as fast.

The above temperature dependent results suggest decoupling of relaxation rates from the macroscopic solvent viscosity. This becomes even more apparent when the activation energy (E_a) associated with the medium viscosity is compared to that obtained from temperature dependent average solvation and rotation times of C153 in these media. Table III summarizes the E_a values (see Fig. S5 for the relevant Arrhenius plots)[58] which clearly show that even in PEG (in the absence of electrolyte) activation energies different from those associated with viscosity regulate the solvation and rotation processes of a dipolar probe dissolved in it. Interestingly, addition of electrolyte decreases the E_a associated with solute solvation and rotation even though the reverse happens for E_a associated with medium viscosity. This suggests a strong role for electrolyte in solute solvation and rotation in these media where the decoupling of whole body polymer motion is augmented via direct participation of ions in excited solute's relaxation processes. In addition, activation energy for solvation in these polymer-electrolyte composites is smaller than that for rotation and these activation energies decrease with increase of K^+ concentration in the composite. This hints at a greater decoupling of solvation than rotation from medium viscosity and greater availability of K^+

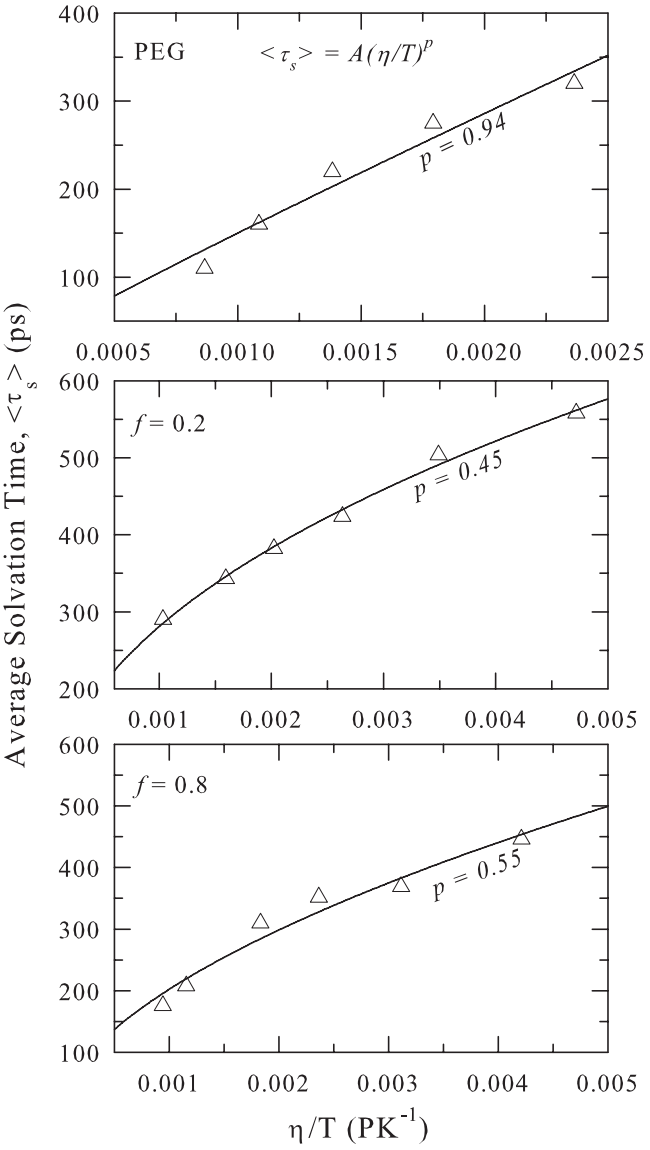

FIG. 6. Plots of average solvation time, $\langle\tau_s\rangle$, versus temperature-reduced viscosity, η/T, obtained from measurements using C153 in PEG and in [0.85PEG + 0.15{f KNO$_3$ + (1−f) LiNO$_3$}] composites at $f = 0.2$ and 0.8. Triangles represent measured data and solid lines represent the best fits through the data points to the relation $\langle\tau_s\rangle = A(\eta/T)^p$. Upper panel represents experimental results in PEG, middle and lower panels represent the same in presence of electrolyte but with differing f values. The fraction power, p, obtained from the fitting is also indicated in the respective panels.

(due probably to its relatively weaker complexation ability) in these polymer-electrolyte composites.

The decoupling phenomenon discussed above is more vivid in Fig. 6 where the dependence of average solvation time ($\langle\tau_s\rangle$) on temperature-reduced viscosity (η/T) is shown for PEG in the absence of electrolyte and PEG-electrolyte composites at $f = 0.2$ and 0.8. Note $\langle\tau_s\rangle$ in polymer-electrolyte composite exhibits a fractional viscosity dependence, $\langle\tau_s\rangle \propto (\eta/T)^p$, but nearly follows the hydrodynamics ($p = 1$) in the absence of electrolyte. Solute rotation in these media, presented right after this discussion, also shows similar fractional viscosity dependence. Note that the fraction power (p) is smaller ($p = 0.45$) at $f = 0.2$ than that ($p = 0.55$) at $f = 0.8$, suggesting stronger temporal heterogeneity in Li^+

enriched composite. This corroborates well with the conclusion regarding spatial heterogeneity derived from λ_{exc} dependent study of fluorescence emission in these composites (see Fig. 3). Note the above decoupling analysis is based on the viscosity dependence of $\langle\tau_s\rangle$ obtained from the present measurements which have missed ~30% of the full solvation response. Therefore, the extent of decoupling (as transpired by p values) may alter in the case of complete detection of the full dynamics and the subsequent use of "true" $\langle\tau_s\rangle$. However, the qualitative character of the comparison will remain the same because $\langle\tau_s\rangle$ is dominated by the longest time constant of the multi-exponential solvation response which, as suggested by data in Table S4, is at least an order of magnitude slower than the faster one.

2. Dynamic fluorescence anisotropy measurements

To further understand the viscosity coupling of solute-centred dynamics we have carried out dynamic fluorescence anisotropy ($r(t)$) measurements of C153 in PEG and PEG-electrolyte composites at various alkali metal ion concentrations and temperatures. Figure 7 presents the measured $r(t)$ decays at 298 K in PEG and in PEG-electrolyte composite at $f = 0$ and 1. Like in solvation, here also one notices slowing down of solute rotation upon addition of electrolyte in PEG and solute rotation is slower in presence of Li^+ than that of K^+ in the composite. The f dependent $r(t)$ decays are bi-exponential functions of time and the fit parameters describing these decays (summarized in Table S6[58]) indicate these decays are characterized by a component (~40%) with time constant in the ~10–20 ps regime (unresolvably fast for us), followed by a slower one spread over ~2–4 ns. The quality of fits is represented by Fig. S7 provided in the supplementary material.[58] The wide difference between the two time constants in the composites reflects a strong non-exponential nature of the underlying friction because strongly separated timescales have also been obtained in the absence of electrolyte. Note the time constants observed in these anisotropy experiments for PEG in the absence of electrolyte at 298 K are in good agreement with those obtained earlier[31] using the same solute and thus provides additional reliability to these measurements. Fit parameters describing the temperature dependent $r(t)$ decays are summarized in Table S8 which reveal enhancement of average decay rate with increase of temperature but with a sort of decoupling that is not as severe as observed in solvation measurements. For example, in the temperature range 298 K–328 K, the long time constant becomes ~4 times shorter in response to decrease of viscosity by ~3 times for PEG, and ~4 times reduction in viscosity in PEG-electrolyte composites at $f = 0.2$ and 0.8 results into ~3 times shortening of the same time constant.

Figure 8 depicts more clearly the viscosity decoupling of solute rotation where the measured average rotation times

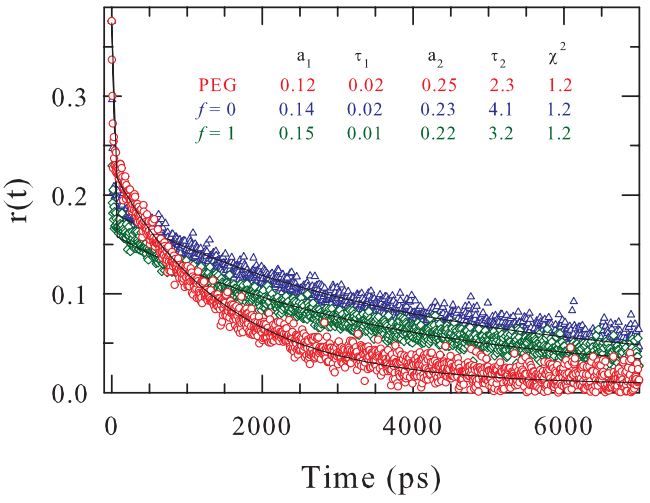

FIG. 7. Effects of electrolyte on dynamic fluorescence anisotropy, $r(t)$, measured using C153 in PEG and in [0.85PEG + 0.15{fKNO$_3$ + (1−f)LiNO$_3$}] composite with $f = 0.0$ and 1.0 at 298 K. Solid lines are the fits through the data. Decay fit parameters are shown in the inset. As before, the time constants (τ_is) are in the unit of nanosecond.

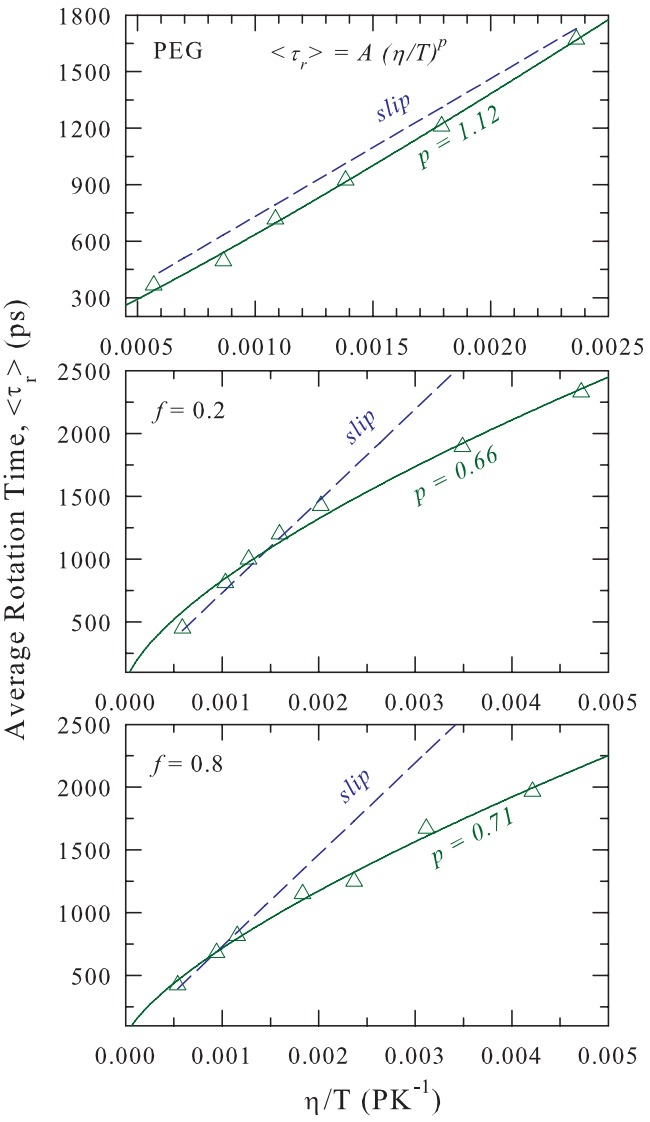

FIG. 8. Plots of average rotation time, $\langle\tau_r\rangle$, versus temperature-reduced viscosity, η/T, for C153 in PEG and in [0.85PEG + 0.15{f KNO$_3$ + (1−f) LiNO$_3$}] composite with $f = 0.2$ and 0.8. Triangles denote measured $\langle\tau_r\rangle$ and solid lines represent best fits through the data to the relation $\langle\tau_r\rangle = A(\eta/T)^p$. p values obtained from the fits are shown in the respective panels. The dashed lines denote slip hydrodynamic limits. Note the stick hydrodynamic predictions are too large to be displayed in the same figure.

($\langle\tau_r\rangle$) are shown as a function of η/T for PEG and PEG-electrolyte composites at $f = 0.2$ and 0.8. Solid lines going through the data points in these panels denote fits denoting power-law dependence of viscosity: $\langle\tau_r\rangle \propto (\eta/T)^p$. As this description demonstrates, presence of electrolyte in PEG renders fractional viscosity dependence to solute rotation in polymer-electrolyte composites. This is similar to the viscosity dependence of solvation times displayed in Fig. 6 with the exception that p values obtained for rotation in these composites are larger (~0.7) than those (~0.5) found in solvation measurements. The kinship to solvation results further grows via near-hydrodynamic ($p \sim 1.1$) dependence of solute rotation in PEG (in the absence of electrolyte), and p being smaller for Li^+ enriched composite than that for K^+ rich solution. Interestingly, similar viscosity decoupling of solute rotation and solvation at high temperature (T ~ 300 K and above) has also been found for deep eutectic multi-component melts[39,41] and is reminiscent of observations in deeply supercooled liquids near glass transition where such decoupling is considered as signature of spatio-temporal heterogeneity.[71–77]

In order to further understand the solute-medium coupling in these complex media, we have calculated the rotation times of solute from the modified Stokes-Einstein-Debye (SED) relation using stick and slip boundary conditions: $\tau_r^h = \frac{V\eta}{k_B T} f_s C$, where V and f_s are the volume and shape factor of solute (C153), respectively, and C is the coupling parameter of solute with surrounding environment.[78,79] We have used $V = 246$ Å^3, $f_s = 1.71$, and $C = 0.24$ (slip boundary condition) and 1 (stick boundary condition).[78] The temperature dependent slip rotation times for PEG and PEG-electrolyte composites (at $f = 0.2$ and 0.8) are shown in the respective panels of Fig. 8 (stick rotation times are too large to be displayed in the same figure). Evidently, measured $\langle\tau_r\rangle$ in PEG are close to the predicted slip rotation times ($\langle\tau_r\rangle \approx \tau_r^h$). Upon addition of electrolyte in PEG, $\langle\tau_r\rangle$ deviates significantly from the hydrodynamic prediction. Presence of spatially heterogeneous micro-environments in polymer-electrolyte composites may be the reason for the observed deviation as similar behaviour has been found in media with known micro-heterogeneity.[80–82]

Next we re-examine the above proposition that presence of micro-heterogeneous environments in polymer-electrolyte composites may be responsible for the observed deviation of measured rotation times from hydrodynamic predictions. This is done by measuring $\langle\tau_r\rangle$ at six different f values at four different temperatures, ~298 K, ~313 K, ~328 K, and ~343 K. The results are shown in Fig. 9 along with the hydrodynamic predictions using slip and stick boundary conditions already discussed. At ~298 K the measured times are approximately 30%–50% faster than the slip predictions at various compositions considered. Upon increase of solution temperature $\langle\tau_r\rangle$ gradually approaches the hydrodynamic slip predictions, τ_r^h. Note we have already observed significant λ_{exc} dependence of C153 emission for the composite with $f = 0.2$ and 0.8 at 298 K (see Fig. 3) and no such dependence at T ≥ 328 K (results not shown). Therefore, $\langle\tau_r\rangle$ approaching τ_r^h with temperature may be considered as a signature of temperature-induced "homogenization" of the composites at higher temperatures. Such an explanation notwithstanding, we would like to mention here that the heterogeneity "observed" here is a direct result of our interpretation of electronic spectroscopy of a dissolved solute which can provide only information about the local environment. The microscopic details of the solution structure of these heterogeneous systems, which remain inaccessible to this technique, are required for a more quantitative description of the observed features. For example, the location of the counter anion with respect to the solute probe can have a direct consequence on the measured spectral shift and dynamics in these composite systems with implications on the observed solute-medium decoupling.

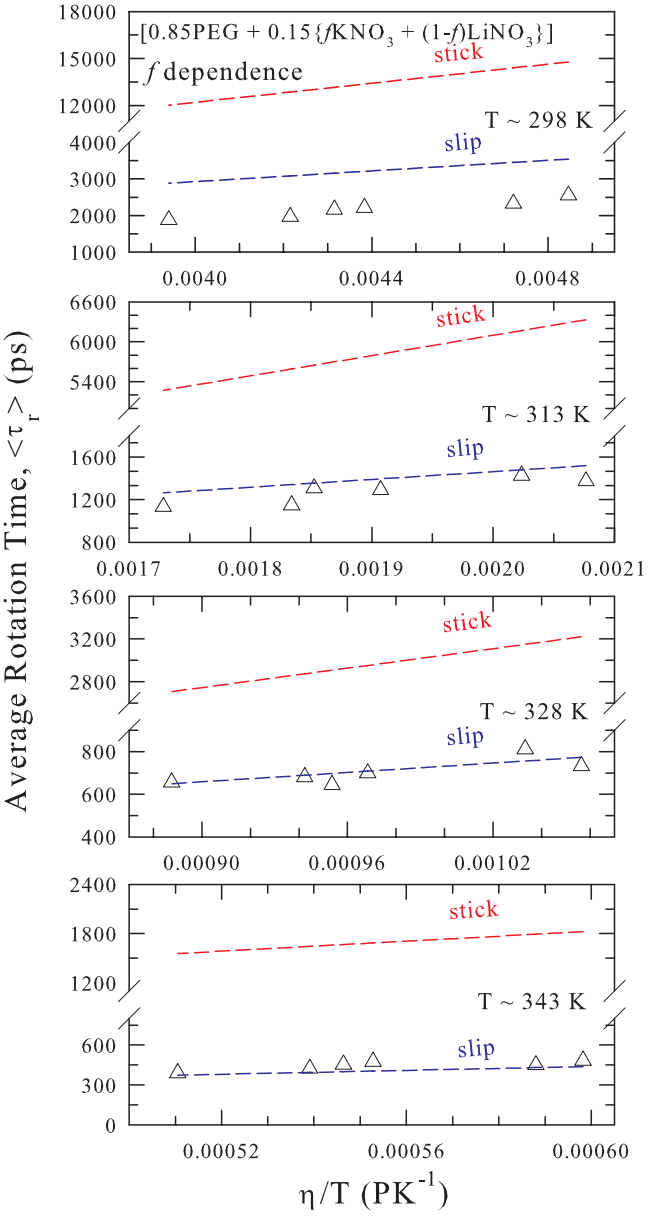

FIG. 9. Electrolyte and fraction of K^+ concentration dependence of $\langle\tau_r\rangle$ at constant temperature for C153 in PEG and in [0.85PEG + 0.15{f KNO_3 + (1−f) $LiNO_3$}] composite. Dependence of measured $\langle\tau_r\rangle$ on f at various temperatures is shown (triangles) in various panels as a function of η/T with T being the temperature mentioned inside a given panel. The dashed lines denote the stick and slip hydrodynamic predictions.

IV. CONCLUSION

To summarize, the work presented here clearly demonstrates creation of spatio-temporal heterogeneity upon addition of electrolyte in PEG300 and substantial reduction or complete removal of it by the increase of solution temperature. Complexation of the PEG molecules with the alkali metal cations and the subsequent formation of micro-domains give rise to the spatial heterogeneity in these polymer-electrolyte composites which have been confirmed via excitation wavelength dependence of the fluorescence emission of a dissolved solute. The arrest or partial quenching of the segmental motion involving $–OCH_2CH_2$ units occurs via this complexation; its effects and those from interactions of metal cations with the end –OH groups of PEG are reflected in the substantial slowing down of the average rates of solvation energy and rotational relaxations ($\langle\tau_s\rangle^{-1}$ and $\langle\tau_r\rangle^{-1}$, respectively) subsequent to photo-excitation. Time-resolved measurements reveal fractional viscosity dependence of average solvation and rotation rates in polymer-electrolyte composites but not in host polymer – an observation consistent with the corresponding steady state photo-selection results. Conformity with the hydrodynamic predictions regarding solute rotation is recovered for these composites by raising solution temperatures. The kind of spatio-temporal heterogeneity observed in these composites is similar to the findings in deep eutectic multi-component melts at high temperature and reminiscent of viscosity decoupling found in deeply supercooled liquids.

Since solvation timescales closely follow the DR timescales, we propose here that the interaction of the metal cations with the end –OH groups should result in lengthening of the slowest DR time observed for PEG300. In addition, relaxation time interpreted as arising from segmental movements should also be severely affected, should the proposed arrest mechanism prevails. The difference in complex formation ability between Li^+ and K^+, as demonstrated via the f dependence of $\langle\tau_s\rangle$ and $\langle\tau_r\rangle$in the present measurements, should also be reflected in DR measurements. The interaction and dynamics in presence of electrolyte of these systems can be studied by employing Kerr spectroscopic measurements. Interestingly, poly(ethylene oxide), or PEO, forms complexes with several electrolytes and the stoichiometry of such complexes depends upon the combination of cation and anion.[83] It would therefore be worth studying whether similar complex formation also occurs for PEG where stoichiometry can be modified via altering the concentration of one of the cations, and such complexes are, in fact, the origin for the observed heterogeneity. Realistic simulation studies of these systems in the presence of cations with varying sizes and charges are required to generate molecular level understanding of complexation and subsequent emergence of heterogeneity in structure and dynamics of these composites.

ACKNOWLEDGMENTS

B.G. acknowledges the Council of Scientific and Industrial Research (CSIR) for providing a research fellowship.

[1] *Application of Electroactive Polymers*, edited by B. Scrosati (Chapman and Hall, London, 1993).
[2] J.-M. Tarascon and M. Armand, Nature (London) **414**, 359 (2001).
[3] A. Barnesy, A. Despotakisy, T. C. P. Wongz, A. P. Andersonz, B. Chambersz, and P. V. Wrighty, Smart Mater. Struct. **7**, 752 (1998).
[4] F. Croce, G. B. Appetecchi, L. Persi, and B. Scrosati, Nature (London) **394**, 456 (1998).
[5] M. Watanabe and N. Ogata, Br. Polym. J. **20**, 181 (1988).
[6] Z. Gadjourova, Y. G. Andreev, D. P. Tunstall, and P. G. Bruce, Nature (London) **412**, 520 (2001).
[7] W. Gorecki, P. Donoso, C. Berthier, M. Mali, J. Roos, D. Brinkmann, and M. B. Armand, Solid State Ionics **28-30**, 1018 (1988).
[8] A. M. Christie, S. J. Lilley, E. Staunton, Y. G. Andreev, and P. G. Bruce, Nature (London) **433**, 50 (2005).
[9] D. Zhou, X. Mei, and J. Ouyang, J. Phys. Chem. C **115**, 16688 (2011).
[10] D. M. Smith, B. Dong, R. W. Marron, M. J. Birnkrant, Y. A. Elabd, L. V. Natarajan, V. P. Tondiglia, T. J. Bunning, and C. Y. Li, Nano Lett. **12**, 310 (2012).
[11] K. Miyatake, Y. Chikashige, E. Highchi, and M. Watanabe, J. Am. Chem. Soc. **129**, 3879 (2007).
[12] S.-Y. Huang, P. Ganesan, S. Park, and B. N. Popov, J. Am. Chem. Soc. **131**, 13898 (2009).
[13] G. S. MacGlashan, Y. G. Andree, and P. G. Bruce, Nature (London) **398**, 792 (1999).
[14] A. Triolo, V. Arrighi, R. Triolo, S. Passerini, M. Mastragostino, R. E. Lechner, R. Ferguson, O. Borodin, and G. D. Smith, Physica B **301**, 163 (2001).
[15] J. W. Halley, Y. Duan, L. A. Curtiss, and A. G. Baboul, J. Chem. Phys. **111**, 3302 (1999).
[16] J. A. Johnson, M.-L. Saboungi, D. L. Price, S. Ansell, T. P. Russell, J. W. Halley, and B. Nielsen, J. Chem. Phys. **109**, 7005 (1998).
[17] F. Muller-Plathe and W. F. van Gunsteren, J. Chem. Phys. **103**, 4745 (1995).
[18] S. Agrawal, M. Singh, M. Tripathi, M. Dwivedi, and K. Pandey, J. Mat. Sci. **44**, 6060 (2009).
[19] S. K. Chaurasia, R. K. Singh, and S. Chandra, J. Polym. Sci., Part B: Polym. Phys. **49**, 291 (2011).
[20] A. Zalewska, J. Stygar, E. Ciszewska, M. Wiktorko, and W. Wieczorek, J. Phys. Chem. B **105**, 5847 (2001).
[21] J. Stygar, A. Biernat, A. Kwiatkowska, P. Lewandowski, A. Rusiecka, A. Zalewska, and W. Wieczorek, J. Phys. Chem. B **108**, 4263 (2004).
[22] P. Carlsson, B. Mattsson, J. Swenson, L. M. Torell, M. Käll, L. Börjesson, R. L. McGreevy, K. Mortensen, and B. Gabrys, Solid State Ionics **113-115**, 139 (1998).
[23] J. P. Donoso, T. J. Bonagamba, H. C. Panepucci, L. N. Oliveira, W. Gorecki, C. Berthier, and M. Armand, J. Chem. Phys. **98**, 10026 (1993).
[24] H.-L. Wang, H.-M. Kao, and T.-C. Wen, Macromolecules **33**, 6910 (2000).
[25] A. Sutjianto and L. A. Curtiss, Chem. Phys. Lett. **264**, 127 (1997).
[26] T. Arimura, D. Ostrovskii, T. Okada, and G. Xie, Solid State Ionics **118**, 1 (1999).
[27] R. Olender and A. Nitzan, J. Chem. Phys. **102**, 7180 (1995).
[28] S. G. Greenbaum, Solid State Ionics **15**, 259 (1985).
[29] Y. S. Pak, K. J. Adamic, S. G. Greenbaum, M. C. Wintersgill, J. J. Fontanella, and C. S. Coughlin, Solid State Ionics **45**, 277 (1991).
[30] G. Mao, R. F. Perea, W. S. Howells, D. L. Price, and M.-L. Saboungi, Nature (London) **405**, 163 (2000).
[31] H. Shirota and H. Segawa, J. Phys. Chem. A **107**, 3719 (2003).
[32] R. Argaman and D. Huppert, J. Phys. Chem. A **102**, 6215 (1998).
[33] T. Sakamaki, T. Fujino, H. Hosoi, T. Tahara, and T. Korenaga, Chem. Phys. Lett. **468**, 171 (2009).
[34] S. Sen, D. Sukul, P. Dutta, and K. Bhattacharyya, J. Phys. Chem. B **106**, 3763 (2002).
[35] S. Ghosh, A. Adhikari, U. Mandal, S. Dey, and K. Bhattacharyya, J. Phys. Chem. C **111**, 8775 (2007).
[36] H. Saito, A. S. Hoffman, and H. I. Ogawa, J. Bioact. Compatible Polym. **22**, 589 (2007); B. Bahmani, S. Gupta, S. Upadhyayula, V. I. Vullev, and B. Anvari, J. Biomed. Opt. **16**, 051303 (2011).
[37] G. Kalita, K. G. Sarma, and S. Mahiuddin, J. Chem. Eng. Data **45**, 912 (2000).
[38] (a) J. Habasaki and K. L. Ngai, Phys. Chem. Chem. Phys. **9**, 4673 (2007); (b) T. Pal and R. Biswas, Chem. Phys. Lett. **517**, 180 (2011).
[39] B. Guchhait, H. A. R. Gazi, H. Kashyap, and R. Biswas, J. Phys. Chem. B **114**, 5066 (2010).
[40] H. A. R. Gazi, B. Guchhait, S. Daschakraborty, and R. Biswas, Chem. Phys. Lett. **501**, 358 (2011).

[41]B. Guchhait, S. Daschakraborty, and R. Biswas, J. Chem. Phys. **136**, 174503 (2012).
[42]M. L. Horng, J. A. Gardecki, A. Papazyan, and M. Maroncelli, J. Phys. Chem. **99**, 17311 (1995).
[43]M. L. Horng, J. A. Gardecki, and M. Maroncelli, J. Phys. Chem. A **101**, 1030 (1997).
[44]R. Biswas, A. R. Das, T. Pradhan, D. Touraud, W. Kunz, and S. Mahiuddin, J. Phys. Chem. B **112**, 6620 (2008).
[45]N. Sarma, J. M. Borah, S. Mahiuddin, H. A. R. Gazi, B. Guchhait, and R. Biswas, J. Phys. Chem. B **115**, 9040 (2011).
[46] (a) V. Ittah and D. Huppert, Chem. Phys. Lett. **173**, 496 (1990); (b) D. Huppert, V. Ittah, and M. Kosower, *ibid.* **159**, 267 (1989); (c) R. Argaman and D. Huppert, J. Phys. Chem. B **104**, 1338 (2000).
[47]C. F. Chapman and M. Maroncelli, J. Phys. Chem. **95**, 9095 (1991).
[48]T. Pradhan, H. A. R. Gazi, and R. Biswas, J. Chem. Phys. **131**, 054507 (2009).
[49]T. Pradhan and R. Biswas, J. Phys. Chem. A **111**, 11514 (2007).
[50]T. Pradhan and Biswas, J. Sol. Chem. **38**, 517 (2009).
[51]S. Schrödle, R. Buchner, and W. Kunz, J. Phys. Chem. B **108**, 6281 (2004).
[52]R. S. Fee and M. Maroncelli, Chem. Phys. **183**, 235 (1994).
[53]H. Jin, X. Li, and M. Maroncelli, J. Phys. Chem. B **111**, 13473 (2007).
[54]A. Samanta, J. Phys. Chem. B **110**, 13704 (2006).
[55]P. K. Mandal, M. Sarkar, and A. Samanta, J. Phys. Chem. A **108**, 9048 (2004).
[56]M. G. McLin and C. A. Angell, J. Phys. Chem. **100**, 1181 (1996).
[57]M. Maroncelli and G. R. Fleming, J. Chem. Phys. **86**, 6221 (1987).
[58]See supplementary material at http://dx.doi.org/10.1063/1.4795583 for static and dynamic spectral properties regarding solute solvation and rotation, time resolved emission spectra, temperature dependent estimated and observed shifts, fit parameters characterizing the solvation response functions and time-resolved anisotropies, composition and temperature dependent viscosity, and Arrhenius plots.
[59]H. Kashyap and R. Biswas, J. Phys. Chem. B **112**, 12431 (2008).
[60]H. Kashyap and R. Biswas, J. Phys. Chem. B **114**, 254 (2010).
[61]A. V. Sarode and A. C. Kumbharkhane, J. Mol. Liq. **164**, 226 (2011).
[62]B. Bagchi and R. Biswas, Adv. Chem. Phys. **109**, 207 (1999).
[63]H. Shirota and H. Segawa, Chem. Phys. **306**, 43 (2004).
[64] (a) T. Fujisawa, K. Nishikawa, and H. Shirota, J. Chem. Phys. **131**, 244519 (2009); (b) H. Shirota, J. Phys. Chem. B **109**, 7053 (2005).
[65]H. Kashyap and R. Biswas, J. Chem. Phys. **127**, 184502 (2007).
[66]D. Pant and N. E. Levinger, Langmuir **16**, 10123 (2000).
[67]B. Bagchi and R. Biswas, Acc. Chem. Res. **31**, 181 (1998).
[68]U. Kaatze, M. Kettler, and R. Pottel, J. Phys. Chem. **100**, 2360 (1996).
[69]B. Zolotov, A. Gan, B. D. Fainberg, and D. Huppert, J. Lumin. **72-74**, 842 (1997).
[70]N. Nandi, S. Roy, and B. Bagchi, J. Chem. Phys. **102**, 1390 (1995).
[71]M. D. Ediger, Annu. Rev. Phys. Chem. **51**, 99 (2000).
[72]H. J. Sillescu, Non-Cryst. Solids **243**, 81 (1999).
[73]M. D. Ediger, C. A. Angell, and S. R. Nagel, J. Phys. Chem. **100**, 13200 (1996).
[74]I. Chang, F. Fujara, B. Geil, G. Heuberger, T. Mangel, and H. Sillescu, J. Non-Cryst. Solids **172-174**, 248 (1994).
[75]C. T. Moynihan, J. Phys. Chem. **70**, 3399 (1966).
[76]C. A. Angell, J. Chem. Phys. **46**, 4673 (1967).
[77]D. Chakrabarti and B. Bagchi, Phys. Rev. Lett. **96**, 187801 (2006).
[78]H. Jin, G. A. Baker, S. Arzhantsev, J. Dong, and M. Maroncelli, J. Phys. Chem. B **111**, 7291 (2007).
[79]C.-M. Hu and R. Zwanzig, J. Chem. Phys. **60**, 4354 (1974).
[80]Y. Miyake, N. Akai, A. Kawai, and K. Shibuya, J. Phys. Chem. A **115**, 6347 (2011).
[81]K. Fruchey and M. D. Fayer, J. Phys. Chem. B **114**, 2840 (2010).
[82]A. L. Sturlaugson, K. S. Fruchey, and M. D. Fayer, J. Phys. Chem. B **116**, 1777 (2012).
[83]M. A. Ratner and D. F. Shriver, Chem. Rev. **88**, 109 (1988).